

Updated: 13 March 2017

Errata and Supplements for the report: **“Polarimetric Upgrades to Improve Rainfall Measurements**; NOAA/NSSL’s WSR-88D Radar for Research and Enhancement of Operations; April 1998.

Preface to this errata and supplements:

The report **“Polarimetric Upgrades to Improve Rainfall Measurements”** has been a useful resource for transferring NSSL research results to the National Weather Service and its contractor Baron Services, Inc. Because the dual polarimetric upgrades have been made by Baron Services to the network of WSR-88D radars at the time of this writing, it seemed useful to update the report with supplements and errata in case users of the data have interest in reviewing the report to learn the underlying engineering results upon which the upgrades have been based. Furthermore, if there are plans to make measurements of the copolar and cross-polar radiation patterns on KOUN after changes have been made by Baron Services, Inc., this updated report could serve as a baseline. The dual pol upgrades made to KOUN by NSSL were to allow radar meteorologists to thoroughly test over a period of years (ca. 2000 to 2010) the performance of the Polarimetric upgrades made to the KOUN before alternative dual pol modifications were made by Baron Services to the fleet of WSR-88Ds.

It is to be noted that the feed horn designed by Andrew Canada and used on the WSR-88Ds prior to conversion to dual-pol system generated a single prominent cross-polar lobe coaxial with the copolar beam. Moreover, Andrew Canada’s dual-pol feed installed on KOUN from ca. 1997-2009 also generated cross-polar fields similar to the single pol feed horn. All measurements made on the KOUN antenna and reported in the NSSL report are those obtain with Andrew Canada’s dual-pol feed. But the Baron Services’ dual-pol feed horn, now installed on all WSR-88Ds, generates a quad of prominent cross-polar lobes having alternating phases and located symmetrically about the copolar beam; moreover the Baron Services’ feed horn produces a null of cross-polar radiation along the copolar beam axis. Nevertheless, the copolar patterns of KOUN should agree with those obtained with the Andrew Canada feed if the aperture illumination is the same.

Thus this report and its errata could be useful for comparisons when and if measurements are to be made on KOUN or any of the WSR-88D after modifications made by Baron Services. The errata and supplemental material listed below is a result of the continuing collaboration and exchange between the Radar Operations Center and NSSL which should keep the 1998 report correct and current.

Page	para.	Line	
4	2	1	here and every else in the text, change 8.53 m to 8.534 m
		4	ditto, change 0.111 m to 0.1109 m
5	1	5-6	change to read: "...are the maximum sidelobe levels specified by Unisys if the antenna is <b>without</b> its radome. Maximum sidelobe levels given by the NEXRAD Technical Specification (NTR) number DV1208252G, plotted in Fig.7.28 of Doviak and Zrnic (1993), are 1 to 4 dB higher than that given in Fig. II.2(b). It is assumed the NTR specification applies to the antenna covered with a radome. Measurements of antenna .....
7	Fig.II.2 (b) caption		change 2 <sup>nd</sup> line to read:"....sidelobe levels <b>without</b> radome."
12	0	6	change to read: '....Thus the scan in Fig.II.4 represents the E plane radiation pattern 0.05° above the principal plane.'
	Fig.II.4(b) caption		at the end of the first line insert "of the antenna without a radome,"
16	1	11	change "might" to "should", and at the end of this paragraph add: "This agreement also suggests that the ad hoc antenna range in Norman is likely suitable for pattern measurements to about the -20 dB level below the radiation peak.
	Fig.II.5 caption		revise second line to "...for the NEXRAD antenna without a radome are given by..."
	Fig.II.6		change the label: "calculated aperture illumination" to "calculated illumination on the reflector". Although both labels are correct, this is not proven until p.26. At this point we have only calculated the illumination on the reflector's surface.
22	3	6	change to read: "... (H, V) copolar and cross-polar fields might not.."
25	3	4	change to read: "would be smaller (smaller) than that measured after the change of...."
		6	change to: "...Although this 0.1° difference is small, it is in a direction one would expect..."

10-12 change the last sentence to read: Moreover, the elevation angle to the radiation source also decreased after the feed change by an about  $0.1^\circ$  (compare.....) as expected if the single port feed was on axis.

25-26 5 change this paragraph to read: “In order to support the deductions that sidelobes along the  $0^\circ$  cut (Fig.II.1a) are principally due to the vertical strut blocking radiation from the aperture, and other anomalous sidelobes are due to scatter from the struts, feedhorn, and imperfections in the parabolic surface, we calculated the sidelobe levels without feed support struts assuming a perfectly made reflector. This calculation gives the radiation pattern outside the ridges of sidelobes due to the feed support struts. We use diffraction theory to compute the ..... (Sherman 1970)”

26 1 1 change to read: “The dashed line in Fig.II.6 is the calculated illumination of the reflector’s surface. This calculation used the feed’s radiation pattern adjusted for the changing distance from the feed to points on the surface. The angle between.....”

2 1-4 change to read: “In general the calculation of the actual radiation pattern requires calculation or measurement of the aperture distribution function and numerical analysis. But, we can obtain an estimate of the radiation pattern by fitting the measured *aperture* illumination function, assumed to be circularly symmetric, with an equation for which a theoretical pattern is known. The theoretical pattern is known if the electric field aperture distribution has the general form (Sherman, 1970, pp.9-21):

Eq.II.1 remains the same

where  $\rho$  is the radial distance.....”

3 because  $\theta$  in this paragraph is different than  $\theta$  on p.27, change  $\theta$  to  $\beta$  everywhere in this paragraph.

3 to clarify the derivation of Eq.(II.2), and to correct an error in computing the secondary radiation pattern, change this paragraph to read:

“The following normalized power density  $S_n(\rho)$  (in dB) across the aperture, as derived from (II.1), is

$$S_n(\rho) = 20 \log_{10} \left[ \frac{(1 - \rho^2 / \rho_o^2)^m + b}{1 + b} \right] \quad (\text{II.2a})$$

To compare this theoretical aperture distribution with that calculated from Fig.II.6, we convert the dependence on  $\rho$  to one on  $\beta$  by substituting  $\rho = (2f / \sin \beta)(1 - \cos \beta)$  to obtain

Equation II.2 is relabeled as (II.2b)

where  $\beta$  is the angle subtended by the line connecting the reflector's vertex to the focus and the line drawn from the focus to a point in the aperture. To relate the electric field incident on the surface of the reflector to the aperture illumination function we use the fact that the amplitude of the field at a point 'A' on the reflector's surface is the same as that in the aperture plane at the point which lies on a line passing through point 'A' and parallel to the axis of the reflector (Fradin 1961, p.381). Thus the calculated aperture illumination function (Fig.II.6), calculated from the measured primary radiation pattern, can be compared with the illumination function  $S_n(\beta)$  across the aperture. That is, the radiation intensity given by the dashed line in Fig.II.6 and the power density given by (II.2) are both the aperture illumination functions. The factor raised to the  $m^{\text{th}}$  power .....and its diameter  $2\rho_o = 853.4$  cm into (II.2b), we have plotted in a **revised** Fig.II.6 the theoretical aperture distribution for  $m = 3$  (the fitting was tested for  $m = 2, 2.5,$  and  $3; m = 3$  produced the best fit to the dashed curve in Fig.II.6 over the angular interval  $\pm 45^\circ$ . This angular interval is where the illumination is most intense. The curves for  $m = 2.5$  and  $2.0$  fit the calculated aperture illumination better near the edge of the reflector, but there the illumination is weakest. It is most important to have the best fit of a theoretical aperture distribution at locations where the illumination is most intense. Furthermore, the aperture distribution with  $m = 3$  matches well the optimized aperture distribution for MPAR (Karimkashi and Zhang, 2012 Fig.9)''

27      1      5      change to read: "...patterns (for  $m = 3,$  and  $b = 0.16$ ) and ...."

Eq.II.3      this equation should be revised to:

$$S(u) = 20 \text{ Log}_{10} \left[ 5.405 \left| 1.68 \frac{4! J_4(u)}{u^4} + 0.16 \frac{J_1(u)}{u} \right| \right] \quad (\text{II.3})$$

where

$$u = \frac{2\pi\rho_o \sin \theta}{\lambda}, \quad 2\rho_o = 8.534, \quad \lambda(\text{KOUN}) = 0.1109 \text{ m}, \quad (\text{II.4})$$

and  $\theta$  is the polar angle measured from the axis of the reflector and a radial to a far field point. This theoretical function ignores changes in sidelobe levels due to the radiation from the reflector being blocked by feed support struts, and reflector surface departure from a parabolic shape. The first term in this equation is the secondary radiation pattern due to the tapered illumination component [i.e., the first term in (II.1)], and the second term is due to the uniform component that illuminates the aperture [i.e., the second term in (II.1)]. The theoretical secondary pattern presented in the revised Fig. II.7 (herein labeled as Fig. II.7a and presented two pages later) is computed using a theoretical primary radiation pattern fitted to the measured primary radiation pattern of the dual polarization feed manufactured by Andrew Canada.

27      2      1-2      change to read: “Eq.II.3 is plotted in the revised Fig.II.7 (now Fig.II.7a) for  $0 \leq \theta \leq 20^\circ$  and compared with the envelope of sidelobes (the dashed-dotted line) deduced from a pattern measured by Andrew Canada (Paramax Report, 1992, p. C-6) along the  $-30^\circ$  cut. All measurements reported herein were made using linear polarization. The  $-30^\circ$  cut was chosen....”

At the end of this paragraph add: But after further study is has been concluded that the asymmetry of the pattern along the  $30^\circ$  cut is due to strut scatter. Strut scatter is shown to be a significant contributor to sidelobes and is discussed in more detail in the errata to pages 28 to 29.

28 → 29 1, 2      replace these two paragraphs with:

The dashed-dotted line is the eye-balled envelope of the sidelobes on the left side of the pattern (p. C-6; Paramax Report, 1992) for the  $-30^\circ$  cut that passes through the region clear of the enhanced sidelobes due to strut blockage (however there is a ridge of sidelobes due strut scatter on one side of the  $30^\circ$  cut pattern—more about that later). The sidelobe slope is approximately 0.4 dB per degree for sidelobes between  $6^\circ$  and  $40^\circ$  (sidelobes between 20 and  $40^\circ$  are not shown in Fig.II.7a—practically all sidelobes measured by Andrew Canada beyond  $20^\circ$  are below the -55 dB level. Theoretical sidelobe levels beyond  $6^\circ$  are principally due to the second term in (II.3). This is the uniform illumination associated with the illumination of the edge of the dish. The higher is the illumination of the edge, the higher are the far out sidelobe levels.

“Figure II.7a also shows measurements of KOUN’s main lobe (i.e., the dots); there is good agreement with the theoretical pattern down to the

-15 or -20 dB level. The three data points (●) are obtained from KOUN pattern measurements after change of feed [i.e., Fig.II.8(c). Antenna range artifacts (i.e., scatter from buildings, terrain, etc.) on NSSL's ad hoc antenna range make it difficult to obtain precise pattern measurements below about -20 dB. For example, an eyeball fit of the envelope of sidelobes along the 0° cut, which are well below -20 dB, needs to be taken with suspicion, even though the measurements are accurate. To emphasize this point Figure II.7b has been added. This figure appears in an NSSL online 2017 Memorandum on "Comparisons of Weather and Aircraft Surveillance Radar Requirements to Determine Key Features for a 10 cm MPAR and SENSR". Figure 7b shows the significantly lower sidelobe level for the 0° cut when measurements were made by Andrew Canada on a better antenna range.

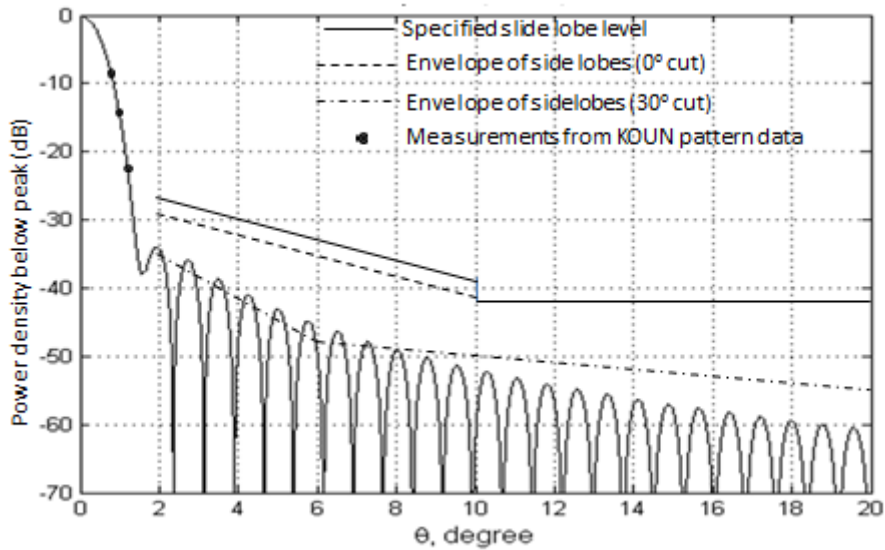


Fig.II.7a KOUN's ( $\lambda = 11.09 \text{ cm}$ ) one-way theoretical copolar radiation pattern (solid wavy line) calculated from (II.3) compared with measurements along various cuts. The dashed line is the envelope of KOUN sidelobes, but the dashed-dotted line is obtained from Andrew Canada pattern data along the  $-30^\circ$  cut with the singularly polarized (H) feed and without radome. The solid lines (i.e., -26 to -38 dB for  $\theta'$  from  $2^\circ$  to  $10^\circ$  and at -42 dB thereafter) are those sidelobe limits specified without radome.

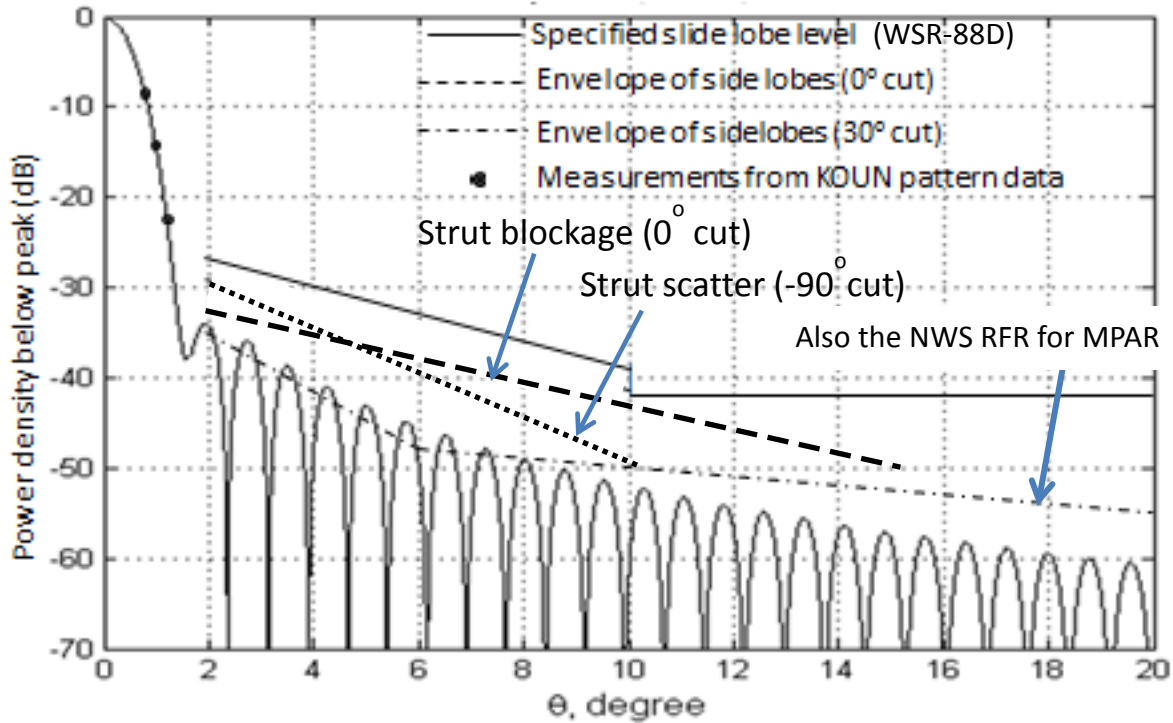


Fig.II 7b The long dashed line is the envelope of sidelobes along the 0° cut as measured by Andrew Canada.

Returning to the discussion of the dashed dotted lines in Fig.II.7a, the -30° cut sidelobe level of the center-fed WSR-88D reflector is practically the same as that obtained for an offset-fed reflector that has no blockage associated with feed support struts (compare Fig.II.7a with Fig.7 of Bringi, et al., JTECH. 2011). Thus the most significant advantage of the offset parabolic reflector is the lack of a ridge of sidelobes due to struts blocking secondary radiation. These heightened levels of sidelobes can cause meteorological measurement error if the ridge of sidelobes illuminates regions of significantly enhanced reflectivity.

Although the envelope of sidelobes for the -30° cut was measured by Andrew Canada—the NSSL antenna range is not designed to make pattern measurements along cuts other than the 0° cut—for a WSR-88D antenna without radome and with the feed generating H linearly polarized radiation, the Andrew Canada sidelobe “pattern” is also representative of the KOUN sidelobe “pattern” with radome and using the dual polarized feed. That sidelobes of KOUN beyond 20° are below -55 dB is supported by KOUN pattern data presented in Fig.II.4a for the 0° cut. Thus, we conclude the KOUN sidelobes outside the regions of enhanced sidelobes

due to struts has a first sidelobe at about -35 dB at 2°, and sidelobe levels decrease linearly in dB to about -48 dB at 6°, and again decrease at a slower rate to about -55 dB at 20°.

We conclude the KOUN sidelobe levels after installation of Andrew Canada’s dual-pol feed horn is the same as that measured by Andrew Canada on a WSR-88D antenna when a single-pol feed horn illuminated the antenna’s reflector—the discrepancies in sidelobe levels measured for KOUN and those measured by Andrew Canada are attributed to the ad hoc range. This conclusion is reasonable and supported by the fact the dual-pol feed is identical to the single-pol feed except an extra port has been added---no change had been made to the conical waveguide and aperture of the feed horn.

The solid lines are the allowed worse case sidelobe levels specified for the antenna **without radome**. These specified levels were given to Andrew Canada (Paramax, 1992), and are 2 dB lower than specified by the NTR for a WSR-88D with radome.

There are six radial ridges of heightened sidelobes due to strut blockage (dashed lines in Fig. II.1a show the locations of the ridges), and each ridge is estimated to have an azimuthal width of about 3°. The significant enhancement of sidelobes due to strut blockage is also clearly seen in the CSU data (i.e., Fig. II.5a). A comprehensive discussion on the ridges of sidelobes generated by strut blockage and scatter is given in annotation (13) of the Memo on MPAR Requirements cited earlier.

29 1 1-9 change to read: “The following formula

$$\theta_1 \approx 1.27 \frac{\lambda}{D} \text{ (rad.)} . \tag{II.5}$$

fits well the one-way beamwidth measurements and the beamwidth obtained from the theoretical radiation pattern (i.e., 0.946° from (II.5) and 0.95° from the theoretical radiation pattern. Although this formula applies well for KOUN at the wavelength of 11.09 cm, this theoretical expression also applies well for the WSR-88Ds operating in the band 11.11 to 10 cm (i.e., 2.7 to 3.0 GHz). For example at  $\lambda = 10$  cm (II.5) gives  $\theta_1 = 0.853^\circ$ ; this compares reasonably well with 0.85° measured by Andrew Canada (Paramax, 1992 pp. C-55, C-57). The Andrew Canada reported beamwidth measurements (i.e., for horizontally polarized waves; the feed used in the legacy radar transmitted only H polarized waves) at each of the selected wavelengths are an average of five measurements made at different cuts across the beam which also showed the beams were circularly symmetric.

Furthermore, measurements made by Seavey Engineering (Baron Radar, 2009, p.22), in 2009 on another WSR-88D reflector illuminated with 11.11 cm H radiation from another dual polarimetric feed gives a beam width of  $0.95^\circ$ , also in good agreement with that derived from the formula. The Seavey feed horn is a dual-pol one and by 2015 all WSR-88D radars have converted to using the Seavey dual-pol feeds. Seavey's beamwidth measurements were obtained from two pattern cuts (i.e., E and H plane cuts---see errata for p.37 for comments on beam circularity). Moreover, because feed horns are different, there is no expectation that the beamwidths measured by Seavey Engineering should be in exact agreement with those measured by Andrew Canada. Nevertheless, based upon the few available data, the theoretical formula  $\theta_1 = 1.27\lambda / D_a$  appears to provide, for the WSR-88D antennas, beamwidths with accuracy better than  $0.1^\circ$  over the entire operating band of frequencies.

The angular diameter  $\theta_0$  of the first null circle (the first null circle is a minimum not a zero) obtained from Fig.II.7a for KOUN is  $3.1^\circ$ . The good agreement of the half power beam width formula for operation in the entire band suggests that the angular diameter of the first null for other WSR-88D radars can be obtained from the formula

$$\theta_0 = 4.16 \frac{\lambda}{D} \text{ (rad)} \quad \text{(II.6)}$$

The angular diameter of the first null circle defines the main lobe or beam of the antenna. Substituting into (II.6) gives  $\theta_0 = 3.10^\circ$  for KOUN.

Comparing with that  $3.45^\circ$  measured by Andrew Canada [i.e., Fig.II.2(b) right panel] and that measured by NSSL for KOUN [i.e.,  $3.56^\circ$  from Fig.II.8(c)], it is seen both independent measurements agree to within 0.1 dB, but differ significantly from the  $3.1^\circ$  obtained from (II.6). The measured null location is subject to significant error because the antenna range is not ideal (i.e., measurements more than 20 dB below the main lobe peak are subject to significant errors induced by scatterers on the antenna range). However the null circle diameter obtained from II.6 is in excellent agreement with the theoretical value of  $3.12^\circ$  obtained by interpolating data in Table 2 of Sherman (1970).

2 delete this paragraph because it no longer applies to the revised Eq.II.3.

32 1 6-8 change  $1.04^\circ$  to  $0.95^\circ$  and delete the last sentence.

34 3 2 change to read: "...illustrates that the cross-polar radiation along the..."

9 add: (4) reflection of the copolar beam from the ground and conversion of H polarization to V polarization (and vice versa) from scatterers on the ground, and (5) as it will be argued in an added comment to text on p.37, the possible generation of the  $TM_{11}$  mode in the feed horn causes the formation of a cross-polar peak along the axis of the copolar beam.

4 6-7 delete "whereas the pattern in .....with a single port feed"

36 1 at the end of this paragraph add:

For example, if the cross-polar and copolar fields are in or out of phase, a null in the on axis radiation would be achieved by rotating the source antenna by  $\frac{\pi}{2} \pm \tan^{-1}(E_{xp} / E_{cp})$  where  $E_{xp}$  and  $E_{cp}$  are the cross-polar and copolar field amplitudes along the boresight. Thus a -32 dB on-axis cross-polar peak could be nulled by a  $1.4^\circ$  tilt of the source antenna, a sufficiently small angle that it might not be noticed by eye. If the cross-polar and copolar were in phase quadrature, a minimum in signal having the magnitude of the cross-polar radiation would be observed. Thus nulling the cross-polar radiation by rotating the source antenna requires measurements of its orientation to insure that nearly pure H and V radiation is transmitted or received along the beam axis. Precise orientation measurements would verify whether the antenna under test is transmitting and receiving nearly pure H and V radiation along the beam axis.

37 at the top of this page insert the following paragraph:

A possible support for the contention that an on-axis peak of cross-polar radiation could exist for the WSR-88D (and perhaps for the CSU antenna), we refer to the work of Potter (1963)<sup>1</sup>. Potter states that in order to obtain circularly symmetric beams for both the H and V polarized waves from a circularly symmetric feed, a  $TM_{11}$  mode should be excited within the throat of the feed. Potter presents radiation patterns of this feed showing excellent symmetry of the copolar radiation pattern. Potter shows that with only  $TE_{11}$  mode excitation, the H plane beamwidth at the -20 dB level is about 1.3 times larger than the E plane beamwidth. On the other hand,

---

<sup>1</sup> Potter, P. D., 1963: A new horn antenna with suppressed sidelobes and equal beamwidths. *The Microwave Journal*, June, pp. 71-78.

there also is a pronounced on-axis peak in the cross-polar radiation! This peak in cross-polar radiation is about 33 dB below the copolar peak, in remarkable agreement with the WSR-88D cross-polar peak observed in Fig. II.6, suggesting the cross-polar peak could be due to a purposely excited  $TM_{11}$  mode in the throat of the WSR-88D feed. But excitation of the  $TM_{11}$  mode is not the only approach to create a circularly symmetric radiation pattern.

In a telecom (c.a., 20??) with Tom Tralman of ASC Signal (formerly Andrew Canada) it was learned Andrew Canada feed horns (scaled versions are used on NSSL's 3-cm and OU's 5-cm radar antennas) are conical **having a single  $TE_{11}$  mode, and a choke flange** that not only reduces currents on the outside of the horn, but also makes the beam more circularly symmetric as seen in beamwidth measurements along five cuts through the copolar beam (Paramax Report, 1992); thus significant cross-polar radiation along the copolar beam axis caused by a  $TM_{11}$  mode in Andrew Canada's feed horns is not likely..

**Therefore it is concluded the prominent cross-polar lobe coaxial with the copolar beam, seen both in Andrew Canada's and NSSL's measurements, is an measurement artifact caused by cross-polar coupling in reflection from the ground when the copolar main lobe is at a low elevation angle needed to make far field pattern measurements at the respective antenna ranges.**

In support of this contention, the cross-polar field measured by Andrew Canada for OU's 5-cm radar antenna exhibits a deep null along the beam axis suggesting its narrower copolar beam (i.e.,  $0.5^\circ$  vs  $1.0^\circ$  for the WSR-88D—Zrnic et al 2010) illuminates the ground more weakly than the broader WSR-88D beam. Moreover, cross-polar pattern measurements made by Seavey Engineering also shows a deep cross-polar null along the copolar beam although the beam width is  $1^\circ$ . Because Seavey Engineering's antenna range has a drop in the terrain between the WSR-88D antenna and the radiation source in the far field, the lack of a cross-polar beam coaxial with the copolar beam in their data can be attributed to weaker ground reflection. Baron Services subcontracted Seavey Engineering to build and test its dual polarimetric feedhorn illuminating a WSR-88D antenna; this feed horn was eventually installed on the network of WSR-88D radars.

The symmetry of WSR-88D radiation patterns measured by Seavey Engineering was also checked. An examination of the 3 dB beamwidths at frequencies between 2.7 and 3.0 GHz suggest that there is less than  $0.1^\circ$  difference in the E and H plane beamwidths. Although measurements along other cuts were not made, the agreement in beamwidths for the two cuts suggests the beam is circularly symmetric. Thus the deep null of the cross-polar field along the beam axis, and the inferred circularly symmetry

of the beam pattern, suggests that the Seavey feed horn design also generates a single  $TE_{11}$  mode and has a choke flange to make the copolar radiation pattern to be circularly symmetric!

**Therefore, it is concluded both Andrew Canada's and Seavey Engineering's feedhorns likely produce radiation from the WSR-88D reflector that has cross-polar fields with a quad of four cross-polar lobes surrounding the copolar beam and a null of cross-polar radiation along the copolar beam.**

1 delete the first sentence **and last** sentence and modify the paragraph to “Comparing the CSU and WSR-88D... beyond  $\pm 9^\circ$ , so we are unable to make comparisons of levels far removed from the main lobe. The significantly higher sidelobe levels of the CSU antenna are simply due to the fact that these higher sidelobes are along a ridge of sidelobes due to strut blockage whereas the WSR-88D radiation field does not have a ridge of enhanced sidelobes along the  $45^\circ$  cut.”

On the other hand, measurements presented by Chandrasekar and Keeler (JTECH, 1993) of copolar fields along a cut between the four struts of NCAR's CP-2 10 cm weather radar show sidelobes to be not significantly lower than along the cuts that contain the ridge of enhanced sidelobe levels due to the struts (compare Figs 4 and 8). This observation suggests that the cause of sidelobes of NCAR's and CSU's antenna being significantly higher than those of the WSR-88D is not associated with struts, but perhaps is rooted in the design of the feed horn's radiation pattern, higher rms errors of the reflector's surface, or the poor performance of their ad hoc antenna range.

2 last line: Change II.6.4 to II.6.7.

39 1 1 change “Section II.3” to “Section II.6.2”

40 1 after paragraph 1, add the following paragraphs: Another interesting feature of the cross-polar field of Fig.II.11 (c) is the absence of a quad of prominent lobes of cross-polar radiation along the  $45^\circ$  lines as suggested by Fradin (1961). That is, center fed parabolic reflector antennas illuminated with linear polarization exhibit a quad of four major lobes symmetrically located around the copolar beam and about a beam away. Because Fig.II.11 (c) shows only the lower half of the radiation pattern, two of the four lobes would have been visible if they had peaks of significant value. The quad of 4 cross-polar lobes with peaks about 27 dB below the copolar peak are seen in the cross-polar measurements made by Raytheon on their competing WSR-88D antenna. Such high peaks, if present in the Andrew Canada design would have been seen in Fig.II.11

(c). On the other hand, simulations of the copolar and cross-polar patterns of the WSR-88D antenna illuminated with linear polarization, and using the aperture distribution computed for the Andrew Canada feed horn, show four significant lobes each -35 dB below the copolar peak (Lei et al., 2015; IEEE TGARS). Practical reflector antennas have circular feed horns transmitting the  $TE_{11}$  mode of radiation which reduces the amplitude of four cross-polar peaks (Fradin; 1961), Thus the differences in levels of cross-polar peaks could be due to differences in the magnitude of the  $TE_{11}$  feed horn field intensity as well as the aperture distribution function. These two factors might account for the absence of prominent cross-polar lobes in Fig.II.11 (c).

- 2 at the end of this paragraph add: On the other hand, because the antenna range is not ideal, achieving a null by rotating the standard gain horn does not necessarily imply that the null is a characteristic of the cross-polar pattern as discussed in the next paragraph,
- 41 0 6 change “less” to “more”
- 7-8 change to: “...a few dB below this level (i.e., -33 dB) could also be in error as mentioned in Sections II.6.5 and II.6.7. Thus it is not surprising that KOUN’s copolar sidelobes....”
- 0 at the end of this paragraph add: “To obtain better measurements of the cross-polar fields, we made additional measurements described in Section II.6.7.
- 42 2 4 change “Section II.6.7” to “Section II.6.6”
- 44 1 2 (Figs.II.13a, b) should be (Figs.II.11a, b).
- 46 1 5 insert after “...dB level.”: The significant differences at azimuths larger than plus/minus  $1^\circ$  could be due to scatter from artifacts (i.e., buildings, utility poles, tress, etc.) associated with the antenna range in Norman,. Also, bear in mind...”
- 10 change to: “...scan for the  $0^\circ$  elevation cut are more likely...
- 11 delete this last line.
- 46 the equation should be placed after the second line of the third paragraph
- 49 2 1 change to read: “Cross-polar radiation (e.g.,  $A_v$ ) combines with copolar

- radiation (e.g.,  $A_H$ ) to form, in general, ....”
- 9 change to: “...(Fig.II.A.1 in which the ellipse collapses to a line for linear polarization).  $\tau$  is positive...”
- 3 1 change to: “..between the vertical (cross-polar) and the horizontal (copolar) fields is not 0...”
- Eq (II.8) the equality symbol should be replaced by an approximation symbol.
- 5 change to: “...Appendix (i.e., Section II.8)...”
- 6 delete the parenthetical phrase.
- 7 change “receiver” to “transmitter”.
- 50 2 3 change to: “...The standard gain horn, transmitting H or V polarized waves, was rotated until a minimum was established in the KOUN’s V or H receive channel. That a minimum was achieved and not a zero (i.e., not a sharp and deep null) suggests the cross-polar field is in phase quadrature to the on-axis copolar field. The amount of ....”
- Fig.II.A.1 replace  $E_{v_0}$  and  $E_{H_0}$  respectively with  $A_v$  and  $A_H$ .
- 55 3 4 change to: ....which RHC (or LHC) was chosen for transmission and LHC (or RHC) was chosen for reception....
- 56 Eq.(III.1) for modifications to this equation if the antenna transmits both copolar and cross-polar waves , see Supplements on pages 240-241 in the errata to the book “Doppler Radar and Weather Observations” Academic Press, 1993. These errata are periodically updated and posted on NSSL’s website at [www.nssl.noaa.gov](http://www.nssl.noaa.gov). In the “Quick Links” box select “Publications” to open the page to select “Recent Books” to find the book and listed Errata for the 3<sup>rd</sup> and 4<sup>th</sup> printings.
- 57 0 5 change “polarizabilities” to “susceptibilities”.
- 11-12 modify these lines to read: “.... the wave normal  $k$ , the apparent canting angle  $\psi$ , the true canting angle  $\psi'$ , and  $\delta$ .”
- 1 12 change to read:....because  $4\pi\langle |s_{hh}|^2 \rangle \equiv \sigma_b$  (McCormick and Hendry, 1975), it is seen....”

- 58 0 1 change to read: “.....scatterer’s properties  $\mathbf{X}$ .”
- 61 4 5 last line change to: “....the incident field. Canting angles are...”
- 62 0 8-9 modify to read: “ $\phi_{DP}$  (radians) is the phase difference between the *scattered* H and V waves incident on the antenna **in absence** of canting angle dispersion  $\sigma_{\psi}^2$  (radians) assuming the phase difference of the H and V waves at the transmitter is zero.  $\ell_{hv}$  ( $\ell_{hv} > 1$ ) is ....*power* loss factor.”
- 1 1 change to: “The transformation matrix  $\mathbf{V}^{(T)}$ , which relates...”
- 2 change to: “...[ $E_{th}$ ,  $E_{tv}$ ] as it leaves the antenna to the polarization state of the scattered field vector [ $E_{rh}$ ,  $E_{rv}$ ] returned to the antenna, is,
- (III.22) delete the first matrix.

After (III.22) insert:

In the balance of section III.1 it is assumed H, V waves are alternately transmitted, but simultaneously received (i.e., the ATSR mode). Assuming there is no cross-coupling within the antenna (i.e., the antenna does not transmit or receive cross-polar fields) and the transmitted field intensities with horizontal or vertical polarization are equal, the normalized signals received are:

$$\begin{bmatrix} V_{rh} \\ V_{rv} \end{bmatrix} = \mathbf{V}^{(T)} \begin{bmatrix} 1 \\ 0 \end{bmatrix} \text{ or } \mathbf{V}^{(T)} \begin{bmatrix} 0 \\ 1 \end{bmatrix}$$

in which the normalized transmitted  $E_{th}$  (i.e.,  $\vec{E}_t^{(h)} = [1, 0]$ ) and  $E_{tv}$  are assumed to have unit amplitudes. Thus voltages [ $V_{rh}$ ,  $V_{rv}$ ] received in the H and V channels are alternately copolar and cross polar. The copolar echoes are used to compute  $\tilde{Z}_{dr}$ , the observed differential reflectivity, and the cross-polar echoes are used to compute  $\tilde{L}dr_{vh}$ , the observed linear depolarization ratio.

(III.23) Modify (III.23) to read as

$$\tilde{Z}_{dr} \equiv \frac{\langle |V_{rh}^{(h)}|^2 \rangle}{\langle |V_{rv}^{(v)}|^2 \rangle} = \dots\dots \quad (\text{III.23})$$

where  $\langle |V_{rh}^{(h)}|^2 \rangle$  is proportional to the mean echo power received in the H

channel when the H transmit port is excited (i.e.,  $\langle |V_{th}^{(h)}|^2 \rangle$  is the copolar echo power), and  $\langle |V_{rv}^{(v)}|^2 \rangle$  is the mean echo power received in the V channel when the V transmit port is excited,  $Z_{dr}$  is the intrinsic.....

8 change to: "... resolution volume), and the diacritical tilde (~) denotes a measured parameter."

9 change to: ".....transmission loss factor. In stratified...."

63 1 1 change  $\tilde{L}DR_{vh}$  to  $\tilde{L}dr_{vh}$

64 0 1 change to read: ...a column vector  $[E_r, E_l]^t$  of the circularly polarized....

2 change to read: ....is the column vector  $[E_h, E_v]^t$  for linearly polarized waves, and....

Eq.III.28 the first and last matrices of this equation should be

$$\begin{bmatrix} 1 & -j \\ 1 & j \end{bmatrix} \dots \dots \dots \begin{bmatrix} 1 & 1 \\ -j & j \end{bmatrix}$$

Eq.III.29 the signs of 'j' need to be changed

65 Eq.III.31 sign of 'j' needs to be changed (note the polarity of 'j' in Eqs.30 and 31 are opposite to that used by Torlaschi and Holt in order to be consistent with the convention chosen in our report)

2 2 change III.3.0 to III.30

Eq.III.32 sign of 'j' in the lower of the two equations needs to be changed

2 5 delete "a solution valid even if drops are not equi-oriented"

Eq.III.33 the 'j' sign multiplying  $\phi_{DP}$  needs to be +, and  $\langle S_{hh} S_{vv}^* \rangle$  should be  $\langle S_{hh}^* S_{vv} \rangle$ .

66 1 1 Change III.3.3 to III.33

Eqs.III.34, 35 make the same changes as done for Eq.III.33

1 13 change III.3.5 to III.35

Eq.III.36 the sign multiplying the *Real part* in the numerator needs to be +

	3	5	change to read: ....., which is often the product of....
67	2	7	change copolar to cross-polar
70	1	8	delete “linear”
83	2	3	modify to read:.....and that all drops are of the same size and shape, and that they do not vibrate nor are they canted within
84	0	9	change to read: Because all drops are identical, the $V_h$ .....
94	Fig. IV.7		change caption to read: ..... $Z_{DR}$ varies from -1 to +3 dB in the .....
95	2	2	change $Z_{DP}$ to $K_{DP}$ at both places
98	Eq.IV.29		change $ \rho_{hvm} $ to $ \rho_{hvm}(0) $ and $\rho_{hv}$ to $ \rho_{hv}(0) $
	1	1	change $ \rho_{hvm} $ to $ \rho_{hvm}(0) $
		2	change $\rho_{hv}$ to $ \rho_{hv}(0) $ ; delete $ \rho_{hv}(0) $ at the beginning of the sentence and change to read: This bias, obtained from (IV.29), is plotted.....
98-100	last line		change to read: ...the added change in $K_{DP}$ would be about $0.03^\circ \text{ km}^{-1}$ ...
100	1	7-8	change to read:.....the capability to simultaneously transmit H, V waves, but to alternately receive the reflected H, V waves in a single receiver through the use of a low power switch; this mode of operation.....
101	Fig. IV.12		labels on some of these figures are incorrect. The dimension of $K_{DP}$ is degree per km; $\rho_{hv}$ has no dimension, and $Z_{DR}$ has dimensions of dB.

List of References      Insert:

Potter, P. D., 1963: A new horn antenna with suppressed sidelobes and equal beamwidths. *The Microwave Journal*, June, pp. 71-78.

Karimkashi, S. and G. Zhang 2012: An optimal design of a cylindrical polarimetric phased array radar for weather sensing. *Radio Sci.*, **47**, RS2017, doi:10.1029/2011RS004753.